

Supporting Information for

**Precision Reactive Species Scavenging Enabled by Engineered
Manganese-Doped Bimetallic MOF for Tailored Stem Cell Fate
Regulation**

*Ziyan Yu,^a Fanghua Zhang,^a Zhe Hao,^a Jinzheng Liu,^a Huan Guo,^a Xiyan Li,^b Ruizhong
Zhang^{*a} and Libing Zhang^{*a}*

^a Tianjin Key Laboratory of Molecular Optoelectronic Sciences, Department of Chemistry, School of Science, Tianjin University, Tianjin, 300072, P. R. China.

E-mail: libing.zhang@tju.edu.cn; zhangrz2019@tju.edu.cn

^b Institute of Photoelectronic Thin Film Devices and Technology, Solar Energy Conversion Center, Key Laboratory of Photoelectronic Thin Film Devices and Technology of Tianjin, Engineering Research Center of Thin Film Photoelectronic Technology of Ministry of Education, Nankai University, Tianjin 300350, P. R. China.

*Corresponding author.

Materials and methods

Chemical and materials.

Zinc nitrate hexahydrate ($\text{Zn}(\text{NO}_3)_2 \cdot 6\text{H}_2\text{O}$, 99%), Manganese(II) nitrate tetrahydrate ($\text{Mn}(\text{NO}_3)_2 \cdot 4\text{H}_2\text{O}$, 98%), and 2-methylimidazole (2-MI, 98%) were purchased from Shanghai Aladdin Industrial Inc. Methanol and tannic acid (TA, 98%) were obtained from Shanghai Macklin Biochemical Co., Ltd. Dexamethasone (Dex, 97%) was provided by Shanghai Beyotime Biotechnology Co. Ltd. All chemicals were used as received without further purification, and ultrapure water was used throughout all experiments.

Apparatus and characterization.

Scanning electron microscopy (SEM) (Hitachi SU8600, Japan) and transmission electron microscopy (TEM) (JEM-2100F, Japan) were used to characterize the different morphology of the nanocomposites. The diameters of the samples were calculated by Image J software (ImageJ 1.54f, USA), and each sample containing at least 100 particles was analyzed from TEM images. The X-ray diffraction patterns of each sample were obtained by X-ray diffraction (XRD) (Bruker D8 Focus, Germany) using a copper target at a generator voltage of 40 kV and a generator current of 40 microamps. The chemical state and composition of the sample were confirmed by X-ray photoelectron spectroscopy (XPS) (Thermo Scientific K-Alpha⁺, USA). The binding energies of the nanocomposites are defined as the C 1s peak at 284.8 eV for the surface adventitious carbon. Inductively coupled plasma-optical emission spectroscopy (ICP-

OES) (Agilent 5800, China) was used to determine the actual Mn content of the sample. The nature and type of bonds present were investigated by a Fourier transform infrared instrument (FT-IR) (Thermo Scientific Nicolet iS5, USA) with a KBr beam splitter. Ultraviolet-visible (UV-vis) spectrophotometers (UV-3600 Plus, Japan) were used to measure the UV-vis absorption spectra of the samples. The Zeta potential of each sample was analyzed by nanoparticle size and Zeta potential analyzer (Zetasizer Nano ZS, UK).

Dex Loading and Release.

The standard curve was established by measuring the UV absorption values of various concentrations of Dex in a methanol solution. The supernatant and washing solutions obtained after centrifugation of the Dex-loaded samples were collected, and the loading content (LC) of Dex in (Mn, Zn)EZIF-8 was calculated using the standard curve and the absorption values of the supernatant.

For the *in vitro* release study of Dex, 200 mg of Dex@(Mn, Zn)EZIF-8 was dissolved in 10 mL deionized water and placed in a dialysis bag with a cutoff molecular weight of 3500 Da. The dialysis bag was then immersed in a beaker containing 200 mL PBS and stirred at room temperature. At various time points, samples of the dialysis solution were collected, and the amount of Dex released into the PBS was monitored using UV-vis spectra.

Cell Culture.

Bone mesenchymal stem cells (BMSCs) were cultured with complete DMEM/F-12 medium (DMEM/F-12 medium contained with 10% fetal bovine serum (FBS), 1% penicillin/streptomycin) at 37 °C in a humidified incubator containing 5% CO₂. To initiate osteogenic differentiation, the medium was changed to osteogenic differentiation medium, which was a complete DMEM/F-12 medium containing 50 µg·mL⁻¹ L-ascorbic acid and 10 mM β-glycerophosphate.

Cell Viability Assay.

BMSCs were inoculated on 96-well plates at 8×10^3 cells per well. After adhering overnight at 37 °C, 0, 20, 40, 60, 80, 100 and 120 µg·mL⁻¹ Dex@(Mn, Zn)EZIF-8 were added, respectively. Subsequently, the cells were incubated under 37 °C for 24, 48 and 72 h. The original medium was removed and replaced with DMEM/F-12 medium contained with 5 mg·mL⁻¹ MTT solution, which was cultured in the incubator for 4 h. The original DMEM/F-12 was discarded and the medium was replaced with 100 µL of DMSO solution. Then, the absorbance values of the mixture at 490 nm were detected using an enzyme-labeled instrument (TECAN Infinite E Plex, Switzerland) to calculate cell viability.

To investigate the cytotoxicity of different materials, BMSCs were added with a density of 5×10^3 cells per well in 96-well culture plates and after adhering overnight, the 100 µg·mL⁻¹ of ZIF-8, (Mn, Zn)ZIF-8, EZIF-8, (Mn, Zn)EZIF-8 and Dex@(Mn, Zn)EZIF-8 were added, respectively, which were cultured for 1, 3, and 5 d in DMEM/F-12 with 10% FBS and 1% penicillin/streptomycin. Cell viability was assessed using

MTT analysis.

BMSCs were seeded at a density of 5×10^4 cells per well in a 24-well plate. Then the $50 \mu\text{g}\cdot\text{mL}^{-1}$ and $100 \mu\text{g}\cdot\text{mL}^{-1}$ of the different materials (ZIF-8, (Mn, Zn)ZIF-8, EZIF-8, (Mn, Zn)EZIF-8, and Dex@(Mn, Zn)EZIF-8) for live/dead staining were added, respectively. After 24 h of co-culture, the samples were processed using the Calcein/PI Cell Viability/Cytotoxicity Assay Kit (Beyotime, China) according to the protocol provided by the manufacturer. All the staining processes were performed under dark conditions. A fluorescence microscope (Nikon ECLIPSE LV100NDA, Japan), equipped with two different filters, was used to observe the samples, allowing differentiation between dead and viable cells.

Cellular uptake of Dex@(Mn, Zn)EZIF-8.

First, 1 mg of Dex@(Mn, Zn)EZIF-8 was dissolved with 1 mg of fluorescein 5-isothiocyanate (FITC) in 1 mL of ultrapure water, which was stirred overnight then centrifuged and washed three times before being resuspended in 1 mL of ultrapure water. BMSCs were inoculated in 35 mm confocal dishes at a density of 1×10^5 cells per well. After adhering overnight, the resulting mixture (FITC-Dex@(Mn, Zn)EZIF-8, $20 \mu\text{g}\cdot\text{mL}^{-1}$) was added into the confocal dishes and cocultured for 2, 4, 6, and 8 h, respectively. Finally, the cells were stained with DAPI, and the images of cellular uptake of Dex@(Mn, Zn)EZIF-8 were captured by a laser scanning confocal microscope (LCSM, Nikon, A1R+, Japan).

Cell Spreading and Adhesion.

BMSCs were seeded in 35 mm confocal dishes at a density of 1.5×10^5 cells per well. After adhering overnight, the original medium was replaced with fresh DMEM/F-12 medium for 6 h, with or without Dex@(Mn, Zn)EZIF-8 ($20 \mu\text{g} \cdot \text{mL}^{-1}$). Following this, H_2O_2 ($200 \mu\text{M}$) was added to the dishes as a stimulus, and the cells were incubated for 2 h. BMSCs treated with PBS served as the control group. After washing with PBS, the samples were fixed with 4% paraformaldehyde (Biosharp, China) at room temperature for 15 min. The cells were then permeabilized with 0.25% Triton-X 100 (Beyotime, China) for 15 min at room temperature and blocked with 2% bovine serum albumin (BSA) for 2 h at 37°C in a humidified incubator. Next, the samples were incubated overnight at 4°C with anti-vinculin antibody (bs-6640R, Bioss, China). After washing three times with PBS, Alexa Fluor 488-labeled Goat Anti-Rabbit IgG (H + L) (bs-0295G-AF488, Bioss, China) was added and incubated for 1 h at 37°C in a humidified incubator. For F-actin staining, the samples were treated with TRITC Phalloidin (Solarbio, China) for 30 min at 37°C . After another round of washing with PBS, the cells were stained with DAPI for 10 min, and images were captured using a laser scanning confocal microscope.

Cell Proliferation.

To assess cellular proliferation activity, cells were inoculated in 24-well plates and allowed to adhere overnight. The medium was then replaced with fresh DMEM/F-12, with or without Dex@(Mn, Zn)EZIF-8 ($20 \mu\text{g} \cdot \text{mL}^{-1}$), and the cells were co-cultured

for 6 h. Following this, H₂O₂ (200 μM) was added as a stimulus to induce oxidative damage, and the cells were incubated for 2 h. BMSCs treated with PBS served as the control group. After culturing for 1, 3, and 5 d, the samples were stained with DAPI, and the cells were counted using an automatic cell counter (SmartCell 200 Plus, China).

Cell Migration.

Cell scratch assays were used to assess the impact of Dex@(Mn, Zn)EZIF-8 on cell migration in the presence of H₂O₂-induced oxidative damage. BMSCs were inoculated in 6-well plates at a density of 3×10^5 cells per well. After achieving a fusion rate of about 90%, the samples were divided into various groups, namely, Control, Dex@(Mn, Zn)EZIF-8 (20 μg·mL⁻¹), H₂O₂ (200 μM) and Dex@(Mn, Zn)EZIF-8 (20 μg·mL⁻¹) + H₂O₂ (200 μM), cultivated in DMEM/F-12 with 1% FBS. After that, the cell scratch tests were performed and cell migration was monitored after 12, 24, and 48 h. To better characterize the effect of the material on cell migration under oxidative damage, for the different samples, three areas were selected at each time point to quantify the area of the scratches, thus calculating the cell migration rate.

Supplementary Experimental Data

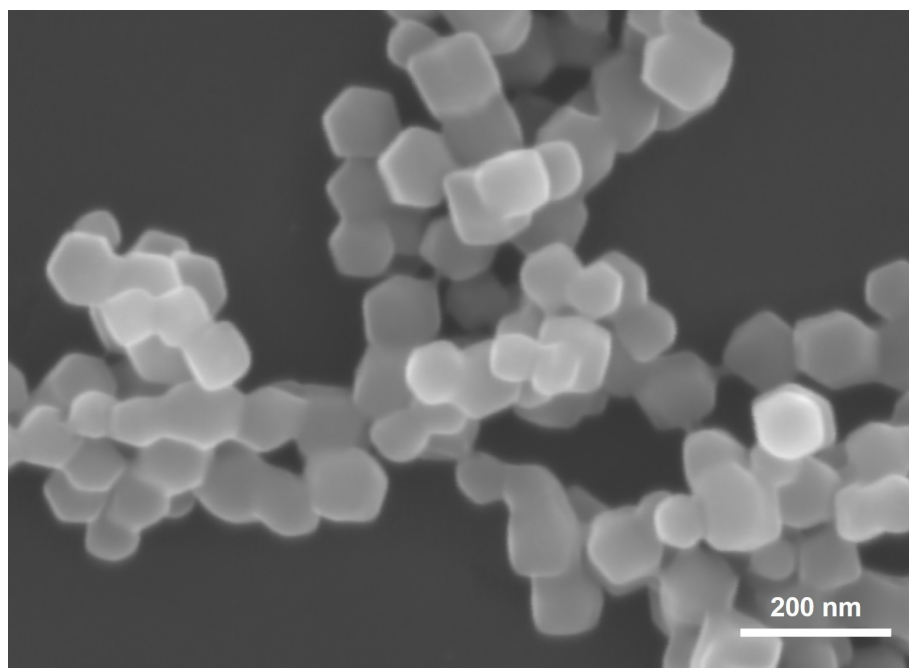


Fig. S1 Morphological and structural characterization of ZIF-8.

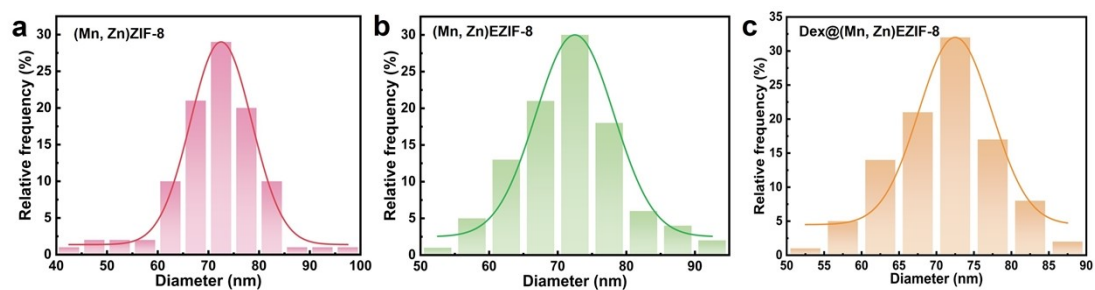


Fig. S2 The granulometric distributions of (a) (Mn, Zn)ZIF-8, (b) (Mn, Zn)EZIF-8 and (c) Dex@(Mn, Zn)EZIF-8.

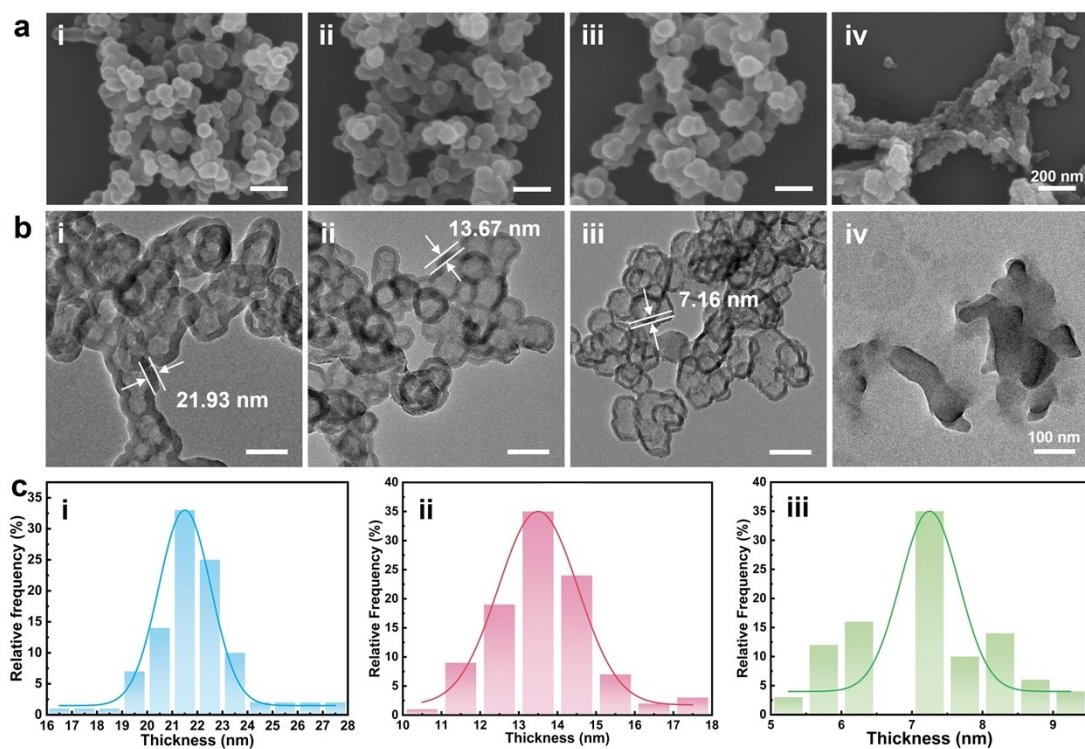


Fig. S3 SEM and TEM images of (Mn, Zn)EZIF-8 after etching at different mass ratios of TA to (Mn, Zn)ZIF-8. (a) SEM of (Mn, Zn)EZIF-8 after etching: 1:0.625 (i), 1:1.25 (ii), 1:2.5 (iii) and 1:5 (iv). (b) TEM of (Mn, Zn)EZIF-8 after etching: 1:0.625 (i); 1:1.25 (ii); 1:2.5 (iii); and 1:5 (iv). (c) The thickness distributions of (Mn, Zn)EZIF-8 after etching: 1:0.625 (i), 1:1.25 (ii), 1:2.5 (iii).

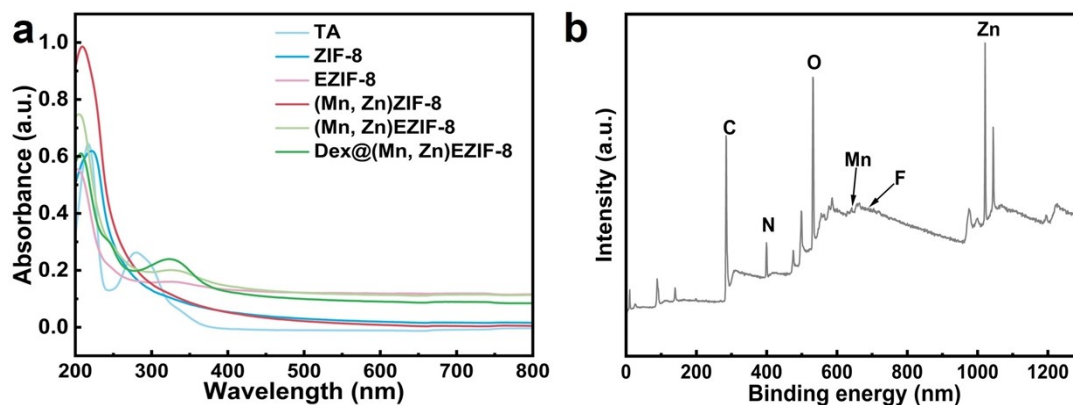


Fig. S4 Characterizations of various nanoparticles. (a) UV-vis spectroscopy of different nanoparticles. (b) Full XPS spectrum of Dex@(Mn, Zn)EZIF-8.

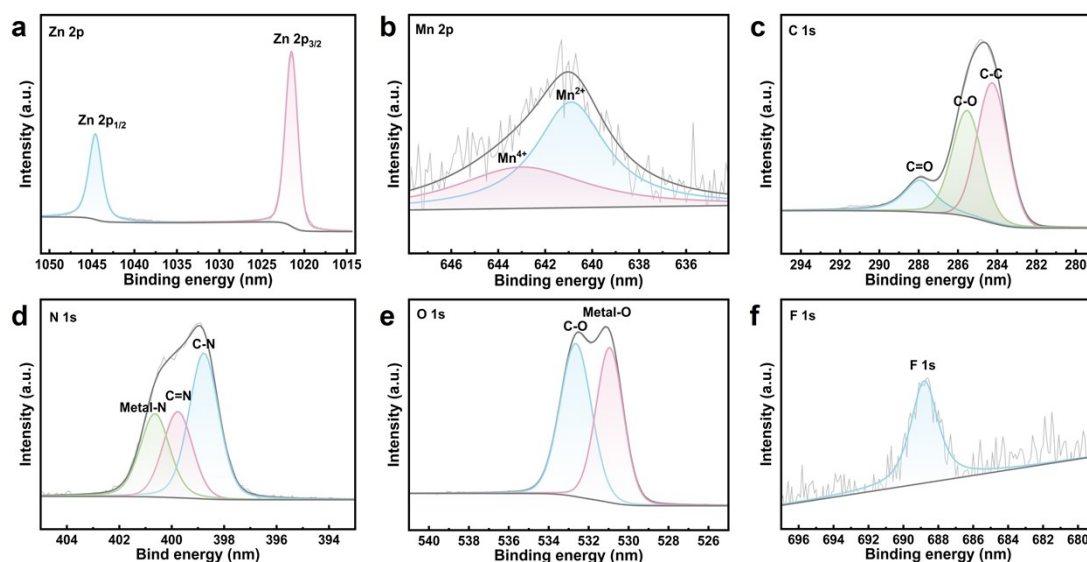


Fig. S5 High-resolution XPS spectra of Dex@(Mn, Zn)EZIF-8. (a) High-resolution XPS Zn 2p spectra. (b) Mn 2p spectra. (c) C 1s spectra. (d) N 1s spectra. (e) O 1s spectra. (f) F 1s spectra.

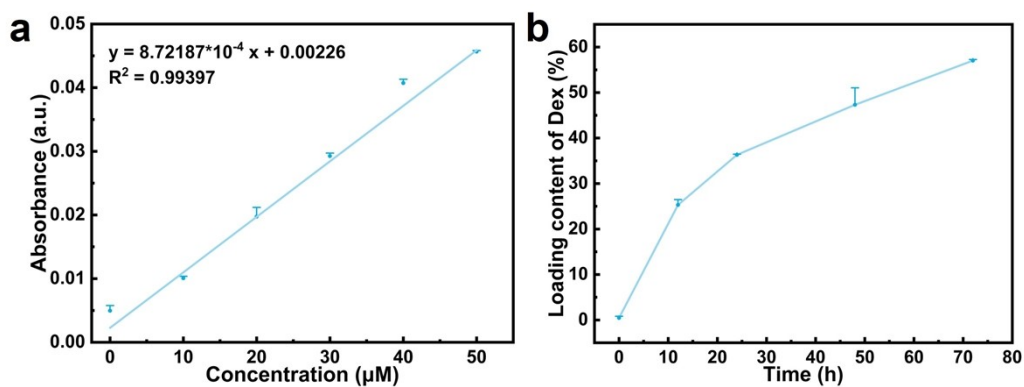


Fig. S6 Loading content of Dex. (a) Standard curve for Dex in methanol. (b) Loading content of Dex in (Mn, Zn)EZIF-8 for 0, 12, 24, 48, 72 h.

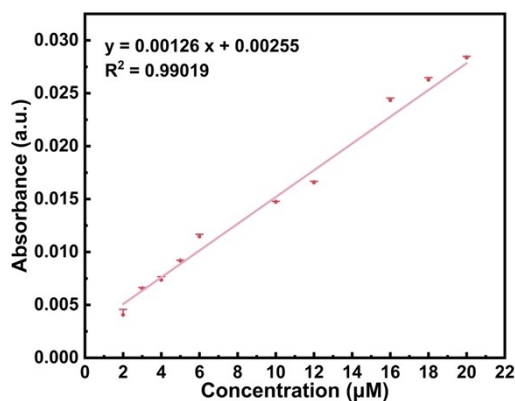


Fig. S7 Standard curve for Dex in PBS.

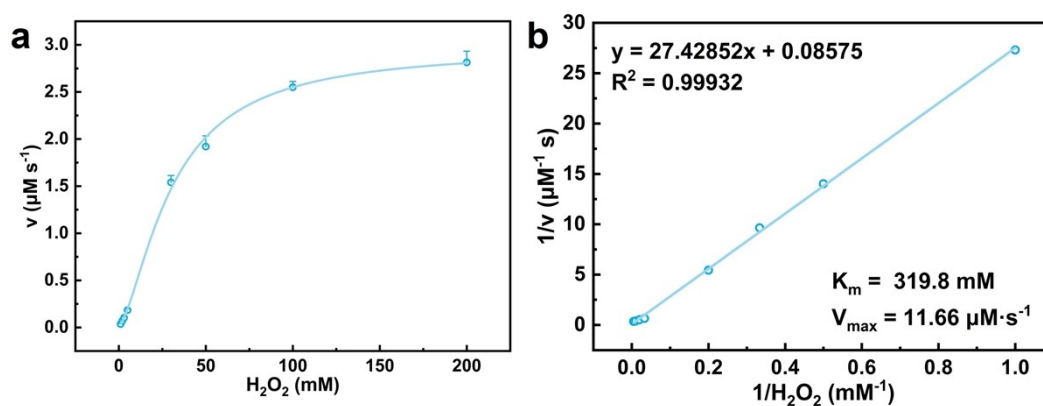


Fig. S8 The steady-state kinetic analysis of CAT-like activity for Dex@(Mn, Zn)EZIF-8. (a) Plot of the velocity of the reaction versus different concentrations of H_2O_2 . (b) The corresponding double reciprocal plot of Dex@(Mn, Zn)EZIF-8.

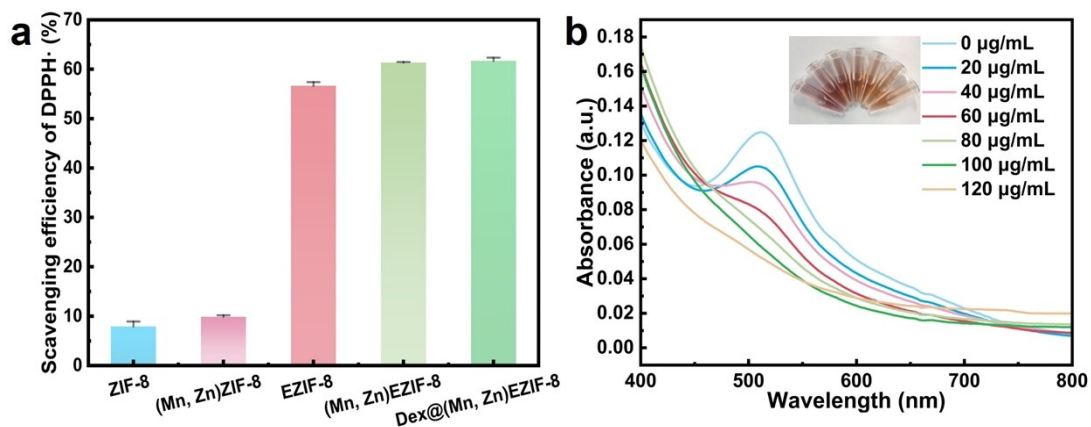


Fig. S9 DPPH• Scavenging activities of Dex@(Mn, Zn)EZIF-8. (a) Scavenging ability of various nanoparticles against DPPH•. (b) Absorbance curves of DPPH• assays for Dex@(Mn, Zn)EZIF-8 at different concentrations.

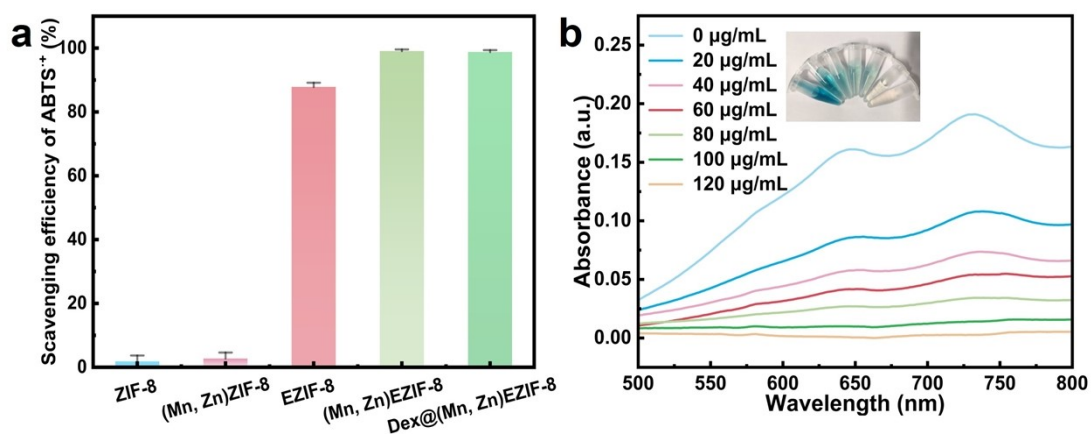


Fig. S10 ABTS•+ scavenging activities of Dex@(Mn, Zn)EZIF-8. (a) Scavenging ability of various nanoparticles against ABTS•+. (b) Absorbance curves of ABTS•+ assays for Dex@(Mn, Zn)EZIF-8 at different concentrations.

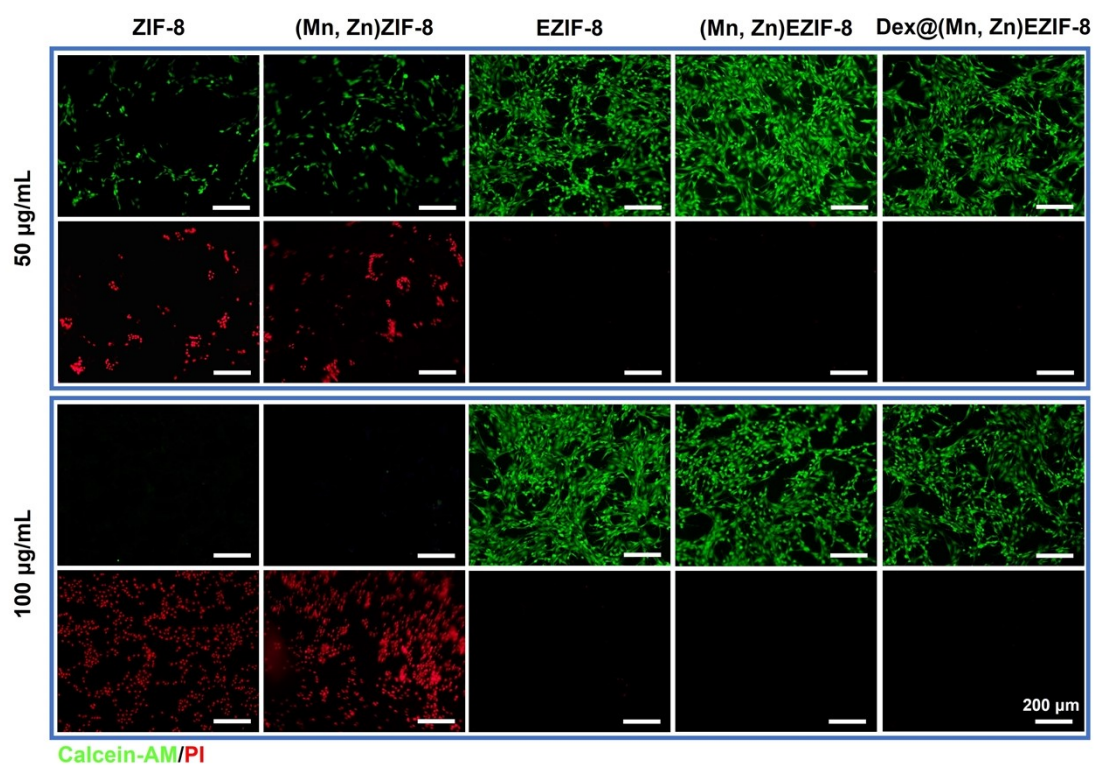


Fig. S11 Live/Dead cell staining of BMSCs after co-cultured with 50 and 100 $\mu\text{g}\cdot\text{mL}^{-1}$ of various materials (ZIF-8, (Mn, Zn)ZIF-8, EZIF-8, (Mn, Zn)EZIF-8 and Dex@(Mn, Zn)EZIF-8) for 24 h; green: live, red: dead; scale bar: 200 μm .

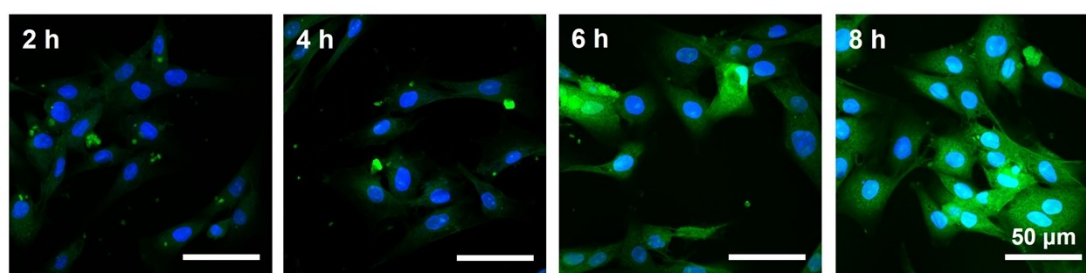


Fig. S12 Cellular uptake of Dex@(Mn, Zn)EZIF-8 after 2, 4, 6 and 8 h of co-culture; green: FITC-Dex@(Mn, Zn)EZIF-8, blue: nuclei; scale bar: 50 μm .

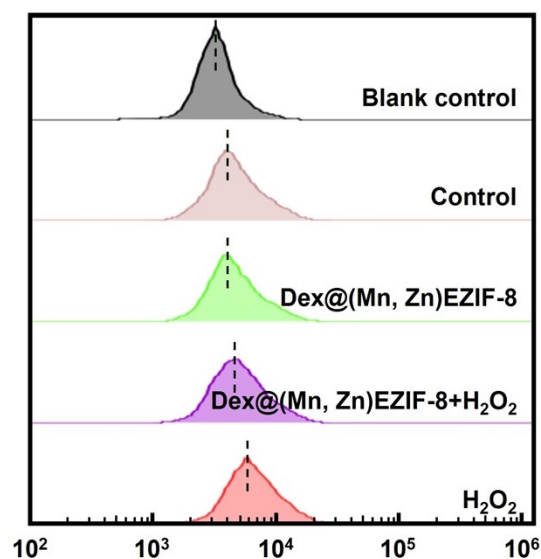


Fig. S13 Flow cytometry of RNS levels in BMSCs under various treatment conditions; Blank Control: untreated cells without fluorescent probes; Control: cells incubated with fluorescent probes but without H_2O_2 stimulation.

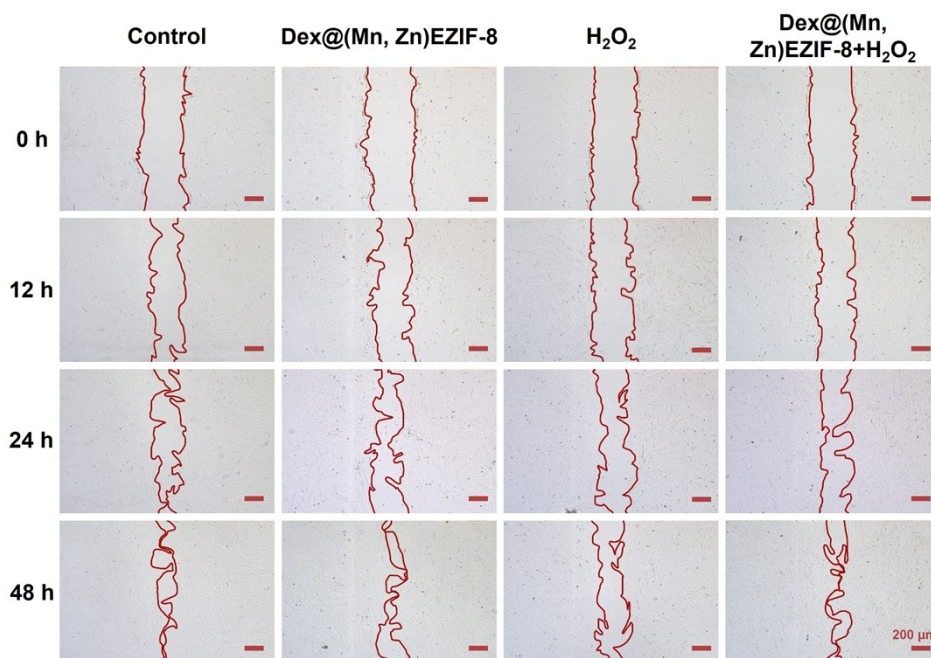


Fig. S14 Representative cell scratch assay images of BMSCs after treatment with PBS, H_2O_2 , Dex@(Mn, Zn)EZIF-8, H_2O_2 + Dex@(Mn, Zn)EZIF-8 for 0, 12, 24 and 48 h; scale bar: 200 μm .

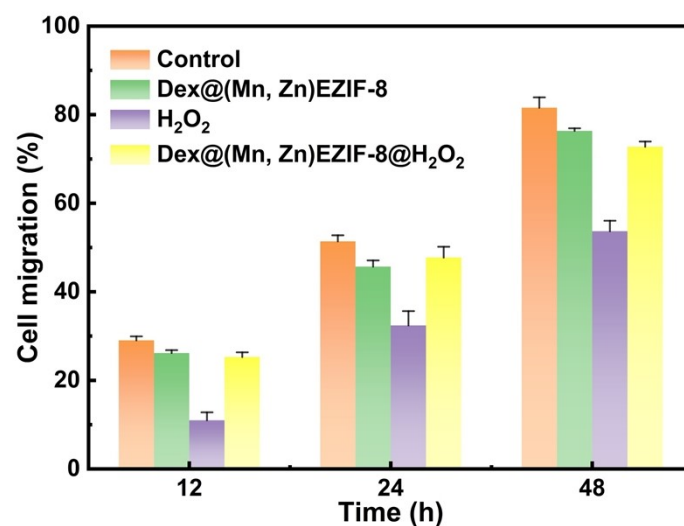


Fig. S15 Quantitative analysis results of cell scratch assay after treatment with PBS, H₂O₂, Dex@(Mn, Zn)EZIF-8, H₂O₂ + Dex@(Mn, Zn)EZIF-8 for 12, 24 and 48 h.

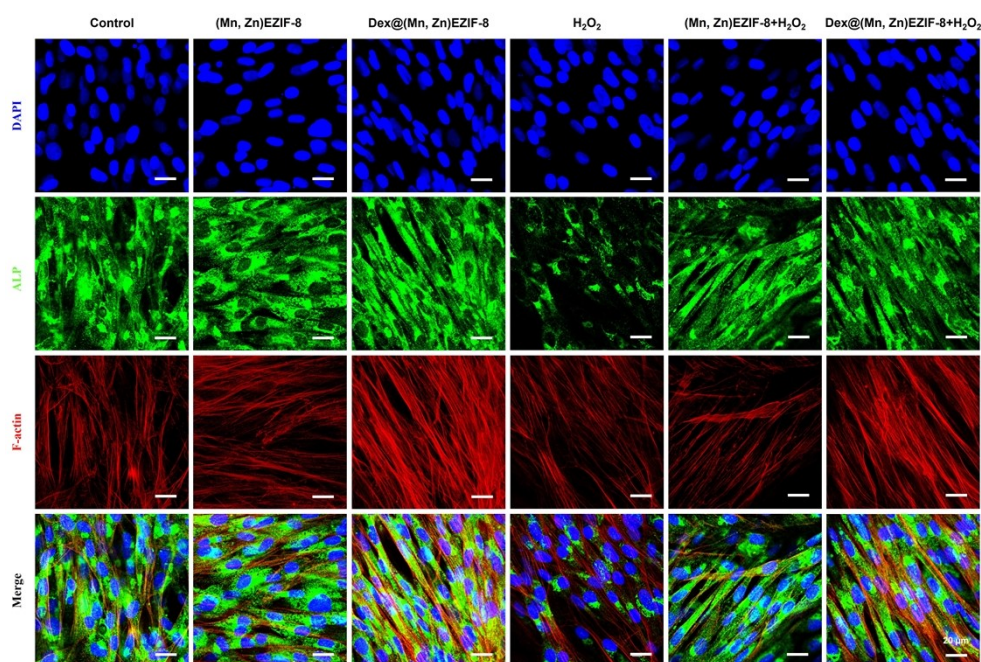


Fig. S16 Representative immunofluorescence images of ALP after 14 d; red: F-actin, green: ALP, blue: nuclei; scale bars: 20 μ m.

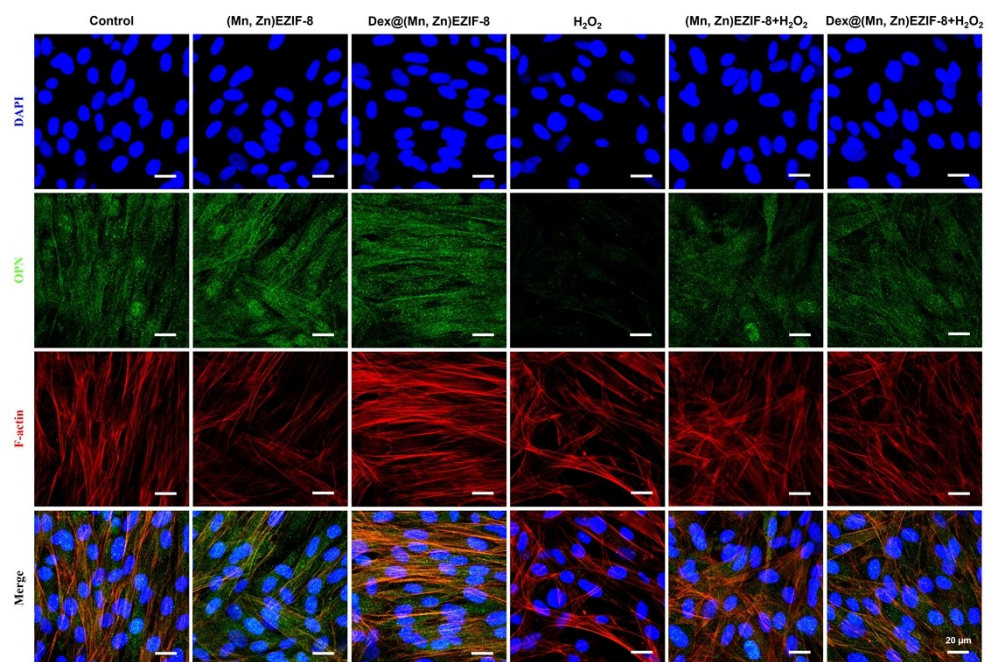


Fig. S17 Representative immunofluorescence images of OPN after 7 d; red: F-actin, green: OPN, blue: nuclei; scale bars: 20 μm.

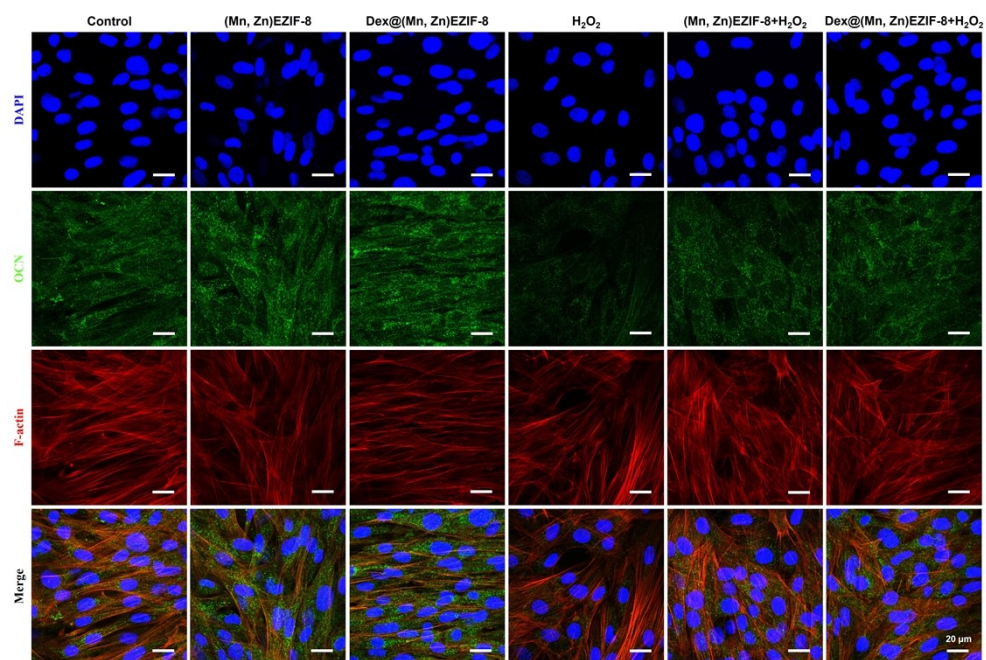


Fig. S18 Representative immunofluorescence images of OCN after 7 d; red: F-actin, green: OCN, blue: nuclei; scale bars: 20 μm.

Table S1. The content of Mn in the Dex@(Mn, Zn)EZIF-8 obtained from ICP-OES.

Element	Concentration (ppm)	Elemental content (%)
Mn	1.74	0.51

Table S2. Comparison of kinetic parameters (K_m , V_{max}) and TON values with recently reported biocatalysts with CAT-like activity.

Sample	K_m (mM)	V_{max} ($\mu\text{M}\cdot\text{s}^{-1}$)	TON (s^{-1})	Refs.
Dex@(Mn, Zn)EZIF-8	319.8	11.66	1.26	This work
MZSO NSs	258.1	0.43	0.017	<i>Adv. Funct. Mater.</i> , 2024, 34 , 2404169.
E-bio-HJ	25.76	1.66	-	<i>ACS Appl. Mater. Interfaces</i> , 2024, 16 , 68950-68966.
$[\text{Mn}(\text{bpia})(\text{OAc})]_2^{2+}$	45	-	0.237	<i>Inorg. Chem.</i> , 2002, 41 , 5544-5554.
$[\text{Mn}^{\text{III}}(2\text{-OHsalpn})]_2$	10.2	-	10.1	<i>Inorg. Chem.</i> , 1998, 37 , 3301-3309.
$[\text{Mn}^{\text{III}}_2(\mu\text{-O})(\text{OH}_2)(\text{OAc})\text{benzimpn}]^+$	6	-	2.7	<i>Inorg. Chem.</i> , 2000, 39 , 3020-3028.
$[\text{Mn}^{\text{III}}_2(\mu\text{-MeO})(\mu\text{-AcO})\text{naphpentO}]^+$	3.5	-	0.79	<i>Inorg. Biochem.</i> , 2006, 100 , 1660-1671.
Mn_3O_4 cubes	0.441	5.30	0.0810	<i>Chem. Eng. J.</i> , 2018, 24 , 8393.
Mn_3O_4 polyhedron	0.613	5.80	0.0886	
Mn_3O_4 hexagonal plates	0.367	7.37	0.1126	
Mn_3O_4 flakes	0.520	21.75	0.3323	

Ligands: *bpia* = bis(picoly)(*N*-methylimidazol-2-yl)amine; *2-OHsalpnH₂* = 1,3-bis(salicylidene-amino)propan-2-ol; *benzimpn* = *N,N,N',N'*-tetrakis(2-methylenebenzimidazolyl)-1,3-diaminopropan-2-ol; *naphpentOH* = bis(2-OH-naphtylidenamino)pentan-3-ol.